Power Balance Models for Rotamak Plasmas

I. J. Donnelly, E. K. Rose and J. L. Cook

Australian Atomic Energy Commission Research Establishment,
Lucas Heights Research Laboratories,
Locked Mail Bag No. 1, Menai, N.S.W. 2234.

Abstract

Energy transfer processes are calculated for a range of rotamak plasmas which are modelled by equilibria with plasma pressure proportional to either the poloidal flux function or the square of this function. The latter case is more realistic, so it is used to study the conditions for which global power balance can be obtained for both the electrons and the ions. The absence of a toroidal magnetic field means that there is no neo-classical transport. Provided that the particle and energy diffusion remains classical when the plasma temperature increases, the energy confinement time is predicted to scale as $n^{3/2} R^8$, where n is the density and R is the radius of the separatrix. As the plasma temperature increases, the dominant energy loss process changes from plasma recycling to electron thermal conductivity and then to ion thermal conductivity.

1. Introduction

The rotamak is a compact torus plasma configuration in which the toroidal current is driven by means of an externally generated rotating magnetic field (Hugrass *et al.* 1980). In this paper, we derive expressions for the various processes which contribute to the power flow in typical rotamak plasmas. The conditions imposed by (i) the magnetohydrodynamic (MHD) equilibrium, (ii) the current drive mechanism and (iii) the global power balance constraints lead to a complete determination of the density and the electron and ion temperature distributions. Therefore, the power flow terms can be evaluated and the dominant ones identified. This knowledge is useful for the interpretation of present experiments and for the planning of future ones.

Since most rotamak experiments have been performed without a toroidal magnetic field, we confine our analysis to this case. This simplifies the calculation of particle and energy diffusion by eliminating neo-classical effects. The oscillating fields associated with the rotating magnetic field (RMF) are expected to affect the plasma equilibrium and the energy transfer processes. The calculation of such effects is difficult, and they are neglected in this paper. In the models considered here the sole effect of the RMF is to drive a rigid-body rotation of the electron fluid, thus giving rise to a toroidal current (Jones and Hugrass 1981).

The plasma configurations studied are the MHD equilibria described by Donnelly, Rose and Cook (1987) (henceforth referred to as DRC). Two types of equilibria are considered, the analytic Solov'ev (1975) model in which the plasma pressure P is proportional to the poloidal flux function Ψ, and the Ψ^2 model for which $P \propto \Psi^2$.

When coupled with the condition that the electron fluid has a rigid-body rotation, the Solov'ev model predicts the plasma density n to be spatially constant, and the temperature T to be proportional to Ψ. In contrast, the Ψ^2 model predicts both n and T to be proportional to Ψ; when the plasma temperature is medium or high, this density distribution is more realistic than the Solov'ev model prediction. Both the Ψ^2 and the Solov'ev models are used to evaluate the energy transfer rates, so that their sensitivity to the density configuration can be assessed. However, only the Ψ^2 model is used for the volume-averaged power balance calculations because the Solov'ev model predicts infinite ohmic heating power at the plasma edge.

Calculations of the thermal energy and particle loss rates for Solov'ev models of compact torus configurations have also been made by Auerbach and Condit (1981) and by Nguyen and Kammash (1982). However, their results and ours cannot be directly compared because of the different density and temperature distributions used. Also of interest is the paper of McKenna *et al.* (1983), who analysed the evolution in time of the energy flows in a cylindrical plasma with a rigid-rotor current distribution. The relevant predictions of this work are in qualitative agreement with our results.

The plan of this paper is as follows. In Section 2, the equilibrium and current-drive conditions are considered. The classical theory of particle diffusion and thermal conduction is presented in Section 3. Expressions for the energy transfer rates are given in Sections 4 and 5. The Solov'ev and Ψ^2 models are compared in Section 6, and scaling laws derived using the Ψ^2 model are presented in Section 7. Sections 8 and 9 describe the power balance studies. The main results and some limitations of the model are discussed in Section 10.

2. The Ψ^2 Model Equilibrium

The Solov'ev and the Ψ^2 model equilibria have been analysed by DRC. We denote the former by the superscript S when they are compared. In this section we summarise relationships between various plasma parameters for the case of the Ψ^2 model equilibrium.

Elsewhere, DRC have solved the Grad–Shafranov equation for a plasma configuration inside an ellipsoidal separatrix defined (in cylindrical geometry) by

$$X^2 + (Z/\zeta)^2 = 1, \tag{1}$$

where $X = r/R$, $Z = z/R$, R is the separatrix radius and ζ determines the separatrix shape. We have $\Psi = 0$ on the separatrix. The pressure distribution is given by

$$P = (2\lambda^2/\mu_0 R^4)\Psi^2, \tag{2}$$

where λ is defined in DRC. For convenience we write

$$\Psi(X, Z) = \psi_0 \psi(X, Z), \tag{3}$$

with ψ normalised to a maximum value of 1.

To evaluate the energy transfer processes, both the number density and the temperature profiles are needed. We consider a hydrogen plasma with $n = n_e = n_i$. The equilibrium equations define the pressure ($P = nkT$ with $T = T_e + T_i$), and two extra relations are required to determine n, T_e and T_i. The 'rotamak condition'

that the electron fluid rotates as a rigid body is used to obtain n and T from P. The values of T_e and T_i can be derived from T by requiring steady-state power balance; we assume that T_e and T_i have the same spatial variation.

In the rotamak, the current is driven by an RMF (with frequency ω) which, in the ideal case, entrains the electron fluid which then rotates as a rigid body (Jones and Hugrass 1981). In low temperature plasmas there is generally some 'slip' between the rotating field and the electron fluid, with the result that the latter rotates at a lower frequency which may vary with position. Here we assume rigid-body rotation at the constant frequency ω. The magnitude of the current density is therefore

$$J_\phi = neR\omega X. \tag{4}$$

Equation (13) in DRC and (4) here give

$$n = n_0 \psi, \quad \text{with} \quad n_0 = 4\lambda^2 \psi_0 / \mu_0 \, eR^4 \omega. \tag{5}$$

If we express T in eV (T^*), the equality $P = neT^*$ and equation (13) in DRC give

$$T^* = T_0^* \psi, \quad \text{with} \quad T_0^* = 0 \cdot 5\omega\psi_0. \tag{6}$$

Thus, both n and T have the same spatial dependence as ψ. We also note that, for a given equilibrium configuration with a fixed toroidal current, n_0 scales inversely and T_0 linearly with ω.

3. Particle and Thermal Energy Fluxes

The evaluation of some energy transfer processes requires a knowledge of the particle loss rate. This is examined together with the related problem of the thermal energy flux. The Ψ^2 model is considered here, and the Solov'ev model is treated in the Appendix.

We use expressions derived from classical particle and energy transport theory (Hinton 1983). Because $B_\phi = 0$, neo-classical effects do not arise. As our main concern is low temperature plasmas, the Coulomb logarithm is assigned the value 10. Unless otherwise specified, we consider a hydrogen plasma ($Z_i = 1$).

The electron and ion particle fluxes perpendicular to a flux surface are related by $\Gamma_e = Z_i \Gamma_i = \Gamma$, with

$$\Gamma = -(\nabla P - 1 \cdot 5 n_e \, k\nabla T_e)/m_e \, \Omega_e^2 \tau_{ei}, \tag{7}$$

where $\Omega_e = eB/m_e$. Note that the gradient terms are all perpendicular to the local flux surface. The electron–ion and ion–ion collision times are (Braginskii 1965)

$$\tau_{ei} = 3 \cdot 5 \times 10^{-10} (T_e^*)^{\frac{3}{2}} (n_e^*)^{-1}, \tag{8}$$

$$\tau_{ii} = 2 \cdot 1 \times 10^{-8} (T_i^*)^{\frac{3}{2}} (n_e^*)^{-1}, \tag{9}$$

where the units of n_e^* are 10^{20} m^{-3}.

The particle flux through the flux surface ψ is

$$\Gamma_t(\psi) = \int_\psi \Gamma \cdot d S. \tag{10}$$

Using the Solov'ev model, Auerbach and Condit (1981) have found $\Gamma_t(\psi)$ as a function of ψ. The evaluation of $\Gamma_t(\psi)$ is difficult for the Ψ^2 model because the flux surfaces and the integrals must be determined numerically. We have, therefore, taken the integral in equation (10) over the surface defined by the separatrix, using the values of $\nabla\psi$ and B at the separatrix but the values of density and temperature on some flux surface ψ. Making use of equation (12) in DRC and

$$|\nabla\psi| = \frac{1}{R}\left\{\left(\frac{\partial\psi}{\partial X}\right)^2 + \left(\frac{\partial\psi}{\partial Z}\right)^2\right\}^{\frac{1}{2}} = RXB\psi_0^{-1} \tag{11}$$

gives

$$\Gamma_t = 1\cdot62\times10^{23}\psi^{\frac{1}{2}}\lambda^2 n_0^*(0\cdot5\,T_{e0}^* + 2\,T_{i0}^*)(T_0^*)^{-1}(T_{e0}^*)^{-\frac{3}{2}}R\mathscr{I}_{tr}, \tag{12}$$

where

$$\mathscr{I}_{tr} = 4\pi\int X^3\left\{\left(\frac{\partial\psi}{\partial X}\right)^2 + \left(\frac{\partial\psi}{\partial Z}\right)^2\right\}^{-\frac{1}{2}}\mathrm{d}l, \tag{13}$$

and the line integral around the separatrix goes from $(X, Z) = (0, \zeta)$ to $(1, 0)$. It is apparent from equation (12) that Γ_t depends only weakly on ψ, except near $\psi = 0$.

We define the particle confinement time to be

$$\tau_p = N/\Gamma_t, \tag{14}$$

where the total number of electrons in the plasma is

$$N = 10^{20}n_0^* R^3\mathscr{I}_{12}. \tag{15}$$

The generalised integral $\mathscr{I}_{mn}$ is defined in equation (26) below.

The thermal energy flux is a sum of thermal conduction and energy convection terms:

$$Q_\alpha = q_\alpha + 2\cdot5eT_\alpha^*\Gamma_\alpha, \qquad \alpha = e, i. \tag{16}$$

In the direction perpendicular to the flux surface we have

$$q_e = -(n_e eT_e^*/m_e\,\Omega_e^2\,\tau_{ei})(4\cdot664e\nabla T_e^* - 1\cdot5n_e^{-1}\nabla P), \tag{17}$$

$$q_i = -(2n_i e^2 T_i^*/m_i\,\Omega_i^2\,\tau_{ii})\nabla T_i^*. \tag{18}$$

The electron thermal conduction and convection terms are of the same order, whereas the ion energy flux is dominated by conduction.

Defining the thermal energy flux through the flux surface ψ by

$$P_{t\alpha} = \int_\psi Q_\alpha\cdot\mathrm{d}S, \tag{19}$$

and using the reasoning that led to equation (12) gives

$$P_{te} = 7\cdot6\times10^4\psi^{\frac{3}{2}}\lambda^2 n_0^*(T_{e0}^*)^{-\frac{1}{2}}R\mathscr{I}_{tr}, \tag{20}$$

$$P_{ti} = 1\cdot6\times10^6\psi^{\frac{3}{2}}\lambda^2 n_0^*(T_{i0}^*)^{\frac{1}{2}}(T_0^*)^{-1}R\mathscr{I}_{tr}. \tag{21}$$

The contribution to P_{ti} of the convection process has been omitted as it is negligible. The approximation $(T_{e0}^* + 0.69\,T_{i0}^*)/(T_{e0}^* + T_{i0}^*) \approx 1$ has been used to simplify expression (20). Note that $P_{t\alpha}$ is more sensitive to the value of ψ than is Γ_t.

The thermal energy content of the plasma is

$$E_\alpha = 24\,n_0^*\,T_{\alpha 0}^*\,R^3\,\mathscr{I}_{14}, \tag{22}$$

and we define the thermal energy confinement times to be

$$\tau_{t\alpha} = E_\alpha/P_{t\alpha}. \tag{23}$$

A question arises concerning the validity of the expressions (7), (17) and (18) near the neutral point, where $B \approx 0$. These expressions are valid provided that $\Omega_\alpha \tau_{\alpha i} \geqslant 3$, otherwise they give values which are too large. In the Appendix we use the Solov'ev model to show that the contribution to $\mathscr{I}_{tr}$ coming from the neutral point is negligible; we have confirmed this numerically for the Ψ^2 model. Therefore, our expressions for Γ_t and $P_{t\alpha}$ are not rendered incorrect by the overestimation of the very small losses in the vicinity of the neutral point.

The values of ψ to be used in equations (12), (20) and (21) are yet to be determined. Assuming edge densities and temperatures which are about 10% of the central values, $\psi = 0.1$ appears to be a reasonable choice if the losses are classical. However, the experience in tokamaks is that both τ_p and τ_{te} are anomalously small, and that they are related by $\tau_p \approx \tau_{te}$ to $5\tau_{te}$ (Hugill 1983). The substitution in equations (12) and (20) of $\psi = 0.5$ (corresponding to an 'average' density and temperature) is probably more realistic than $\psi = 0.1$ because it gives $\tau_p \approx 1.5\tau_{te}$ (for $T_{i0} = 0.5\,T_{e0}$) and leads to enhanced particle and electron thermal energy losses. We do not expect the ion thermal loss rate to differ markedly from the classical value, so equation (21) is evaluated using $\psi = 0.1$. The choice of $\psi = 0.1$ in equation (21) and $\psi = 0.5$ in (12) gives $\tau_p/\tau_{ti} \approx 1$, which is in reasonable agreement with measurements on field-reversed configurations (Hoffman et al. 1984).

Henceforth, we evaluate equations (12) and (20) using $\psi = 0.5$ and (21) using $\psi = 0.1$. This corresponds to an 'enhanced classical' evaluation of the particle diffusion and the electron thermal energy transport, and a classical evaluation of the ion thermal energy transport.

4. Energy Transfer Processes

The volume-integrated power balance equations for the electron and ion components of the plasma are written as

$$\frac{\partial}{\partial t} \int 1.5\,n_e\,e\,T_e^*\,\mathrm{d}V = P_\Omega - P_{ei} - P_{te} - P_{ne} - P_{br} - P_{ec} - P_{lr}, \tag{24}$$

$$\frac{\partial}{\partial t} \int 1.5\,n_i\,e\,T_i^*\,\mathrm{d}V = P_{ei} - P_{ti} - P_{cx}. \tag{25}$$

We consider only the steady-state case, so that the LHS terms are zero. The source terms for electron and ion energy balance are ohmic heating P_Ω and the equilibration

term P_{ei} respectively. The other terms represent energy loss processes. Given a specified plasma equilibrium and defined expressions for each term on the RHS of (24) and (25), the only free parameter that can be changed to satisfy energy balance is T_{e0} which (since $T_{\text{e0}} + T_{\text{i0}} = T_0$ and $T_{\text{i0}} < T_{\text{e0}}$) is restricted to the range $0 \cdot 5 T_0 < T_{\text{e0}} < T_0$. In general, an extra free parameter is needed to allow both electron and ion power balance to be obtained. This requirement has led us to modify both the electron thermal energy flux and the particle loss rate, as discussed below in Sections 4c, 4d and 8.

The evaluation of the energy transfer processes requires volume integrations of functions which depend on density, temperature and position. Many of these integrals can be reduced to the form

$$\mathscr{I}_{mn} = 4\pi \int_0^\zeta \mathrm{d}Z \int_0^{X'} X^m \psi^{n/2} \, \mathrm{d}X, \tag{26}$$

where $X' = \{1 - (Z/\zeta)^2\}^{1/2}$. All the Ψ^2 model energy transfer integrals are evaluated in Section 5.

For the Ψ^2 model, the RHS terms of (24) and (25) are given by the following expressions. The Solov'ev model is treated in the Appendix.

(a) Ohmic Heating

Writing the (perpendicular) resistivity as

$$\eta = 1 \cdot 05 \times 10^{-3} (T_{\text{e}}^*)^{-\frac{3}{2}}, \tag{27}$$

gives the ohmic heating power as

$$P_\Omega = \int \eta J_\phi^2 \, \mathrm{d}V = \{4 \cdot 15 \times 10^{-2} (T_{\text{e0}}^*)^{-\frac{3}{2}} \mathscr{I}_{31} / R \mathscr{I}_{12}^2\} I_\phi^2. \tag{28}$$

(b) Electron–Ion Energy Transfer

The energy equilibration is (Braginskii 1965)

$$P_{\text{ei}} = \int 3(m_{\text{e}}/m_{\text{i}}) n_{\text{e}} \tau_{\text{ei}}^{-1} e(T_{\text{e}}^* - T_{\text{i}}^*) \, \mathrm{d}V$$

$$= 7 \cdot 47 \times 10^7 (n_0^*)^2 (T_{\text{e0}}^*)^{-\frac{3}{2}} (T_{\text{e0}}^* - T_{\text{i0}}^*) R^3 \mathscr{I}_{13}. \tag{29}$$

(c) Electron Thermal Energy Loss

The thermal energy loss P_{te} is derived from equation (20) with $\psi = 0 \cdot 5$. We also introduce a scaling factor α into the expression for P_{te}, so that both electron and ion power balance can be satisfied:

$$P_{\text{te}} = 2 \cdot 7 \times 10^4 \alpha \lambda^2 n_0^* (T_{\text{e0}}^*)^{-\frac{1}{2}} R \mathscr{I}_{\text{tr}}. \tag{30}$$

The method for evaluating α is discussed in Section 8.

(d) Electron Energy Used to Ionise Neutral Particles

For plasmas in thermal equilibrium, the energy associated with ionisation and recombination is negligible for plasma temperatures greater than a few eV. However, equation (14) indicates that the particle confinement time can be very short ($<100\ \mu s$) for low temperature plasmas, so the observation that the density remains fairly constant during rotamak discharges, which typically have duration times of 10 ms (Durance *et al.* 1987), implies that the plasma is continually refuelled by an influx of neutral particles which are ionised at a rate equal to Γ_t. These neutrals are probably H atoms and H_2 molecules which are formed by recombination at the vessel wall, so we assume that the bulk of the neutrals have energies well below 1 eV because of wall effects. Relaxation of this assumption would not change the loss given in equation (31) below by more than $\sim 50\%$. There are many competing processes involved in the ionisation of H and H_2. Using the cross sections referenced by Dolan (1982) we estimate that, for the low temperature plasma configurations considered here, low energy neutrals penetrate (on average) to where the plasma temperature is about 10 eV before they are ionised. Before ionisation, the neutrals are excited by electron collisions and radiate a quantity of energy which is dependent on the plasma density and the electron temperature (Harrison 1984). We estimate that, for cases in which this energy loss channel is important, the electron energy lost through line radiation and ionisation of the incoming neutrals is about 50 eV per ionisation, so that the total energy loss is

$$P_{ne} = 50 e \Gamma_t. \tag{31}$$

For future reference, we define the number density of H atoms to be n_n, equate the total ionisation rate to Γ_t and use the fact that the ionisation rate at $T_{e0}^* \approx 10$ eV is $\langle v_e \sigma_{ion} \rangle \approx 2 \times 10^{-14}\ \mathrm{m}^3\,\mathrm{s}^{-1}$ to derive

$$\int n_e n_n\, dV \approx 5 \times 10^{13}\, \Gamma_t. \tag{32}$$

We derive Γ_t from equation (12) with $\psi = 0 \cdot 5$, and with the scaling factor α included so that the ratio of τ_p to τ_{te} remains constant:

$$\Gamma_t = 1 \cdot 15 \times 10^{23} \alpha \lambda^2\, n_0^* (0 \cdot 5\, T_{e0}^* + 2\, T_{i0}^*)(T_0^*)^{-1}(T_{e0}^*)^{-\frac{3}{2}} R \mathscr{I}_{tr}. \tag{33}$$

(e) Bremsstrahlung

A volume integration of the expression given by Dolan (1982) for power radiated as bremsstrahlung gives

$$P_{br} = 150 Z_{eff}(n_0^*)^2 (T_{e0}^*)^{\frac{1}{2}} R^3 \mathscr{I}_{15}. \tag{34}$$

In all calculations we take $Z_{eff} = 1$.

(f) Electron Cyclotron Radiation

By assuming an optically thin plasma and no wall reflection, the electron cyclotron radiation power is given by (Miyamoto 1980)

$$P_{ec} = 6 \cdot 2 \int B^2 n_e^* T_e^* \, dV = 6 \cdot 2 \times 10^{-5} \lambda^{-2} (n_0^*)^2 T_{e0}^* T_0^* R^3 \mathscr{I}_{ec}, \qquad (35)$$

where

$$\mathscr{I}_{ec} = 4\pi \int_0^\zeta dZ \int_0^{X'} X^{-1} \left\{ \left(\frac{\partial \psi}{\partial X} \right)^2 + \left(\frac{\partial \psi}{\partial Z} \right)^2 \right\} \psi^2 \, dX. \qquad (36)$$

For the configurations considered here, B^2 is small where nT is large and vice versa, which decreases the cyclotron radiation, compared with the case of nearly constant magnetic field.

(g) Line Radiation

We consider the line radiation from an oxygen impurity with number density $n_{ox} \propto n_e$. With a corona equilibrium model the line radiation power is

$$P_{lr} = 10^{40} f_{ox} (n_0^*)^2 R^3 \mathscr{I}_{lr}, \qquad (37)$$

where

$$f_{ox} = n_{ox}/n_e,$$

$$\mathscr{I}_{lr}(T_{e0}, \zeta) = 4\pi \int_0^\zeta dZ \int_0^{X'} X R_{ox}(T_{e0} \psi) \psi^2 \, dX, \qquad (38)$$

and R_{ox} is the radiation power function which we derive from Post *et al.* (1977). In all calculations we take $f_{ox} = 0 \cdot 03$, unless otherwise stated. The only appreciable line radiation from hydrogen is that associated with the incoming neutrals; this is already included in (31).

(h) Ion Thermal Energy Loss

The ion thermal energy loss P_{ti} is given by equation (21) with $\psi = 0 \cdot 1$.

(i) Charge Exchange Losses

By assuming thermal neutrons and no re-ionisation of the charge exchange neutrals, the power loss due to this process is

$$P_{cx} = \int e T_i^* n_e n_n \langle v_i . \sigma_{cx}(T_i) \rangle \, dV. \qquad (39)$$

For atomic hydrogen, we have $\langle v_i \sigma_{cx} \rangle \approx 10^{-14} (T_i^*)^{1/4} \text{ m}^3 \text{ s}^{-1}$ when $1 < T_i^* < 10^4$ (Dolan 1982). The evaluation of (39) requires a knowledge of the distribution of neutrals throughout the plasma. This is not known, so we note the discussion in Section 4*d* and assume an average value for T_i^* of $(T_{i0}^*/T_{e0}^*) \min(10, T_{e0}^*)$. Thence, use of equation (32) gives

$$P_{cx} = e(T_{i0}^*/T_{e0}^*) \min(10, T_{e0}^*) \Gamma_t. \qquad (40)$$

This formulation probably underestimates the charge exchange losses from hot plasmas. A comparison of equations (40) and (16) shows that $P_{cx} \ll P_{ti}$; therefore, the charge exchange losses are negligible.

Table 1.   Energy transfer integral coefficients

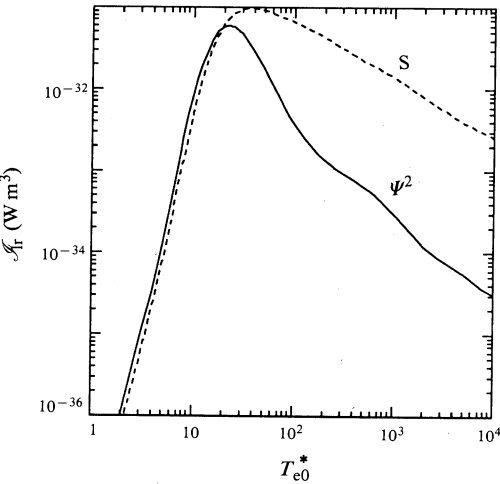| Term	$\mathscr{I}(1)$	a	b	Term	$\mathscr{I}(1)$	a	b
$\mathscr{I}_{12}$	1·50	0·83	0·13	$\mathscr{I}_{31}$	0·99	0·89	0·08
$\mathscr{I}_{13}$	1·12	0·81	0·14	$\mathscr{I}_{tr}$	3·52	2·34	−1·40
$\mathscr{I}_{14}$	0·90	0·80	0·14	$\mathscr{I}_{ec}$	9·50	0·30	−0·14
$\mathscr{I}_{15}$	0·74	0·80	0·15	$\mathscr{I}_{lr}$	$\mathscr{I}_{lr}(T_{e0}^{*})$	0·79	0·15

Fig. 1. Oxygen line radiation power integral against the electron temperature for the Ψ^2 and Solov'ev models.

5.   Power Transfer Integrals

In Section 4 the energy transfer rates have been expressed in terms of dimensionless volume and surface integrals which are functions of ζ. For $0 \cdot 5 \leqslant \zeta \leqslant 2$, the transfer integrals are given accurately by functions of the form

$$\mathscr{I}(\zeta) = \mathscr{I}(1)\zeta^{a-b\ln\zeta}. \tag{41}$$

The coefficients $\mathscr{I}(1)$, a and b are listed in Table 1.

The line radiation $\mathscr{I}_{lr}$ is a function of both ζ and T_{e0}; to a good approximation (errors near the peak values are $<10\%$) we write

$$\mathscr{I}_{lr}(\zeta, T_{e0}) = \mathscr{I}_{lr}(T_{e0})\zeta^{a-b\ln\zeta}. \tag{42}$$

A tenth order polynomial in $\ln(T_{e0})$ is fitted to $\ln\{\mathscr{I}_{lr}(T_{e0})\}$ over the range $1 \leqslant T_{e0} \leqslant 1$ MeV, and this is used in the power balance calculations. A plot of $\mathscr{I}_{lr}$ versus T_{e0} is shown in Fig. 1. Note that the peak value occurs when $T_{e0} = 23$ eV, which is only slightly above the temperature at which $R_{ox}(T_{e0})$ is a maximum.

6. Comparison of the Solov'ev and Ψ^2 Model Power Terms

The major difference between the particular Solov'ev and Ψ^2 model equilibria considered in this paper is that the former has constant n, whereas the latter has $n \propto \psi$. This can lead to a considerable difference in individual power densities near the plasma edge. However, in many cases the volume integral of the power is dominated by the contribution from the region around the magnetic axis, so both models predict similar values. Notable exceptions are P_Ω which is infinite in the Solov'ev model, and the particle and thermal energy fluxes which have different dependences on the particular ψ used for their evaluation. If $\psi = 0 \cdot 5$, the two models give similar values for P_{te} and for Γ_t (provided that $T_e \leqslant T_j$). In contrast, we have $P^S_{ti} \approx 100 P_{ti}$, if $\psi = 0 \cdot 1$ is used.

The integral $\mathscr{I}_{tr}$ increases more strongly with ζ than does $\mathscr{I}^S_{tr}$. This occurs because, for $\zeta > 1$, the Ψ^2 model magnetic field on the separatrix is considerably smaller than B^S when $|Z| > \zeta^{1/2}$ (DRC). We note that the contribution to $\mathscr{I}_{tr}$ from the region of small X is negligible, although its percentage value is larger than for $\mathscr{I}^S_{tr}$. A comparison of the flux contours in Fig. 2 of DRC indicates that, inside and on the $\psi = 0 \cdot 1$ contour, the $\nabla\psi$ and $\nabla\psi^S$ fields are alike. Therefore, we expect that $\mathscr{I}_{tr}$ and $\mathscr{I}^S_{tr}$ would have similar values, and a similar dependence on ζ, if evaluated around the $\psi = 0 \cdot 1$ contour. We conclude that our method of evaluating $\mathscr{I}_{tr}$ for the Ψ^2 model leads to an overestimate of the transport losses when $\zeta > 1$.

The oxygen line radiation predicted by the two models is compared in Fig. 1. The Solov'ev model gives a broader peak as expected from a comparison of equations (38) and (A11).

From these comparisons we conclude that, given the condition that the electron fluid has a rigid-body rotation, the Ψ^2 model gives a better description than the Solov'ev model of the plasma density and, therefore, of many of the energy transfer processes. Therefore, we use the Ψ^2 model for the following power balance calculations.

We note that, if the rigid-rotor constraint is removed, the density and temperature in the Solov'ev model can be of the form $n = n_0 \psi^\delta$ and $T = T_0 \psi^{1-\delta}$ ($0 \leqslant \delta \leqslant 1$); Auerbach and Condit (1981) and Nguyen and Kammash (1982) have used this general form to analyse some of the energy transfer processes. The formulation developed in the Appendix is easily extended to this more general equilibrium.

7. Analytic Scaling Relations

In experiments there is a certain amount of control over the values of ω and n_0, so it is useful to express other quantities as functions of these parameters. Using expressions given in DRC and in Section 4, we find that

$$T^*_0 = 2 \cdot 5 \times 10^{-6} \omega^2 n^*_0 R^4 \lambda^{-2}, \tag{43}$$

$$I_\phi = 2 \cdot 5 \omega n^*_0 R^3 \mathscr{I}_{12}, \tag{44}$$

$$\psi_0 / R^2 = 5 \cdot 0 \times 10^{-6} \omega n^*_0 R^2 \lambda^{-2}, \tag{45}$$

$$P_\Omega = 6 \cdot 8 \times 10^7 \omega^{-1} (n^*_0)^{\frac{1}{2}} (T^*_0 / T^*_{e0})^{\frac{3}{2}} R^{-1} \lambda^3 \mathscr{I}_{31}. \tag{46}$$

The term ψ_0 / R^2 is the factor which scales the normalised magnetic field shown in Fig. 1 of DRC.

We define an energy confinement time τ_E which is based on the assumption that the total energy losses are balanced by the ohmic heating power:

$$\tau_E = (E_e + E_i)/P_\Omega$$

$$= 8 \cdot 9 \times 10^{-13} \omega^3 (n_0^*)^{\frac{3}{2}} (T_{e0}/T_0)^{\frac{3}{2}} R^8 (\mathscr{I}_{14}/\lambda^5 \mathscr{I}_{31}). \qquad (47)$$

We have found that, in most cases, the ohmic heating is sufficient to balance the energy loss processes considered in this paper. If large 'anomalous' losses occur, the actual energy confinement time is less than expression (47) and the configurations considered here could only be achieved with additional heating.

The scaling of the above terms with ω, n_0 and R is obvious. In particular we note the strong dependence of τ_E on R. The term $\mathscr{I}_{14}/\lambda^5 \mathscr{I}_{31}$ has the values $3 \cdot 5 \times 10^{-4}$, $1 \cdot 1 \times 10^{-3}$ and $1 \cdot 7 \times 10^{-3}$ when $\zeta = 0 \cdot 5$, 1 and 2 respectively; this demonstrates the weak dependence of τ_E on ζ, especially when $\zeta > 1$.

We anticipate the results obtained in Sections 8 and 9 by observing that, in general, P_{te} and P_{ei} dominate the electron energy loss. It is therefore of interest to consider the ratios

$$P_{te}/P_\Omega = 0 \cdot 25 \alpha (T_{e0}/T_0)(\mathscr{I}_{tr}/\mathscr{I}_{31}), \qquad (48)$$

$$P_{ei}/P_\Omega = 7 \cdot 0 \times 10^2 \, n_0^* \{(T_{e0} - T_{i0})/T_0\} R^2 (\mathscr{I}_{13}/\lambda^2 \mathscr{I}_{31}). \qquad (49)$$

Note the remarkable result that, apart from the factor T_{e0}/T_0, P_{te}/P_Ω is independent of ω, n_0 and R. Thus the 'enhanced classical' electron thermal energy loss rate and the ohmic heating power are always of similar magnitude. The same conclusion holds for P_{ti} and P_Ω when $T_i \sim T_e$. The Ψ^2 model predicts that the term $\mathscr{I}_{tr}/\mathscr{I}_{31}$ has a strong ζ dependence, so that α also has a strong dependence on ζ in those cases for which $P_{te} \approx P_\Omega$.

Equation (49) indicates that P_{ei}/P_Ω is proportional to $n_0^* R^2$ when this parameter is small. As $P_{ei} < P_\Omega$, it is evident that $T_i \rightarrow T_e$ when $n_0 R^2$ becomes large. Also, P_{ei}/P_Ω has only a weak dependence on ζ.

8. Power Balance Survey

The interpretation of many of the results presented in this section is aided by observing that, for given ω, R and ζ, both I_ϕ and T_0 are proportional to n_0.

For a given configuration, the equilibrium and current-drive constraints fix all parameters except T_{e0}, which lies in the range $0 \cdot 5 T_0 < T_{e0} < T_0$. Since $P_{cx} \ll P_{ti}$ in all cases considered, the ion power balance equation becomes $P_{ei} = P_{ti}$, from which T_{e0} can be found. To achieve electron power balance we have scaled the electron thermal flux and the particle flux by the required factor α, which is incorporated in the expressions for P_{te} and P_{ne} in Section 4. We have adjusted P_{te} and P_{ne} because the expressions for these terms have the greatest uncertainty. Also, P_{te} and P_{ne} depend on the values of ∇T_e and ∇n near the plasma edge, and α indicates the changes in these terms needed to give electron power balance.

Figs 2–6 show the dependence on density of α and T_{e0} for a range of ω, R and ζ values. For the majority of cases we have $0 \cdot 3 < \alpha < 1$. In these cases the unadjusted ($\alpha = 1$) expressions (30) and (31) give electron thermal energy loss rates and particle loss rates which are of the correct order of magnitude needed to satisfy power balance.
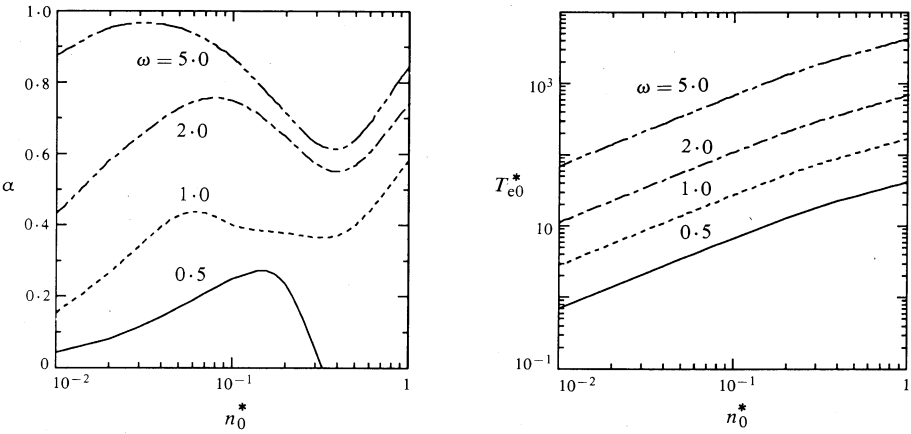
Fig. 2. Dependence of α and T_{e0}^* on n_0^* for $R = 0.2$ m, $\zeta = 1$ and the indicated values of ω (in 10^6 rad s^{-1}).
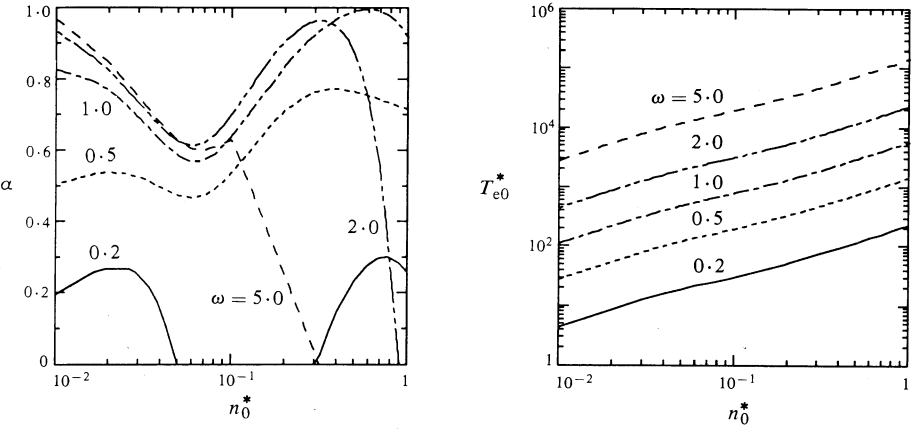
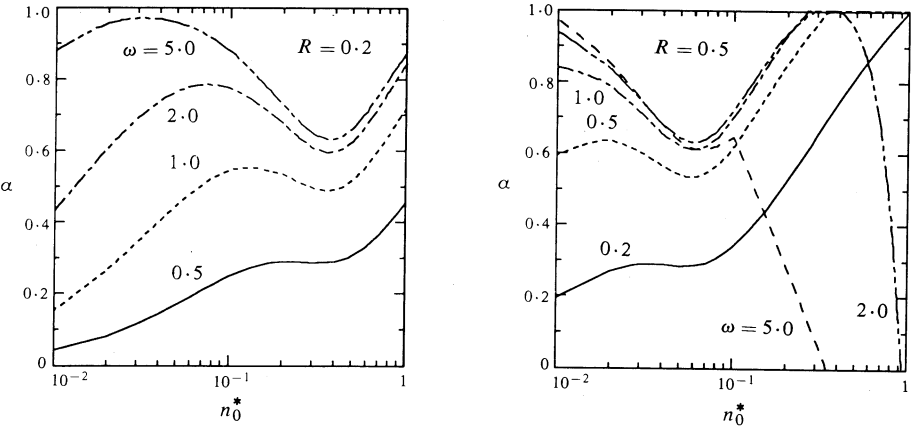**Fig. 3.** The same as Fig. 2 except $R = 0.5$ m.

Fig. 4. Dependence of α on n_0^* for $R = 0.2$ and 0.5 m, for $\zeta = 1$, for zero oxygen line radiation and for the indicated values of ω (in 10^6 rad s^{-1}).
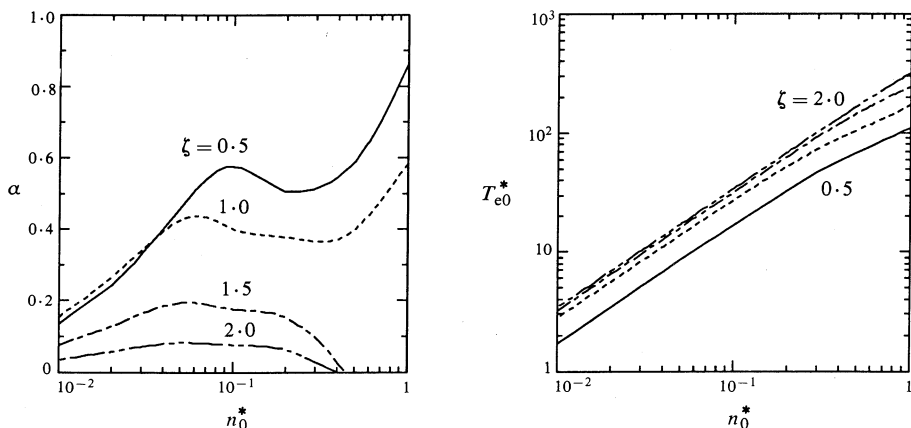
Fig. 5. Dependence of α and T_{e0}^* on n_0^* for $R = 0 \cdot 2$ m, $\omega = 10^6$ rad s^{-1} and the indicated values of ζ.
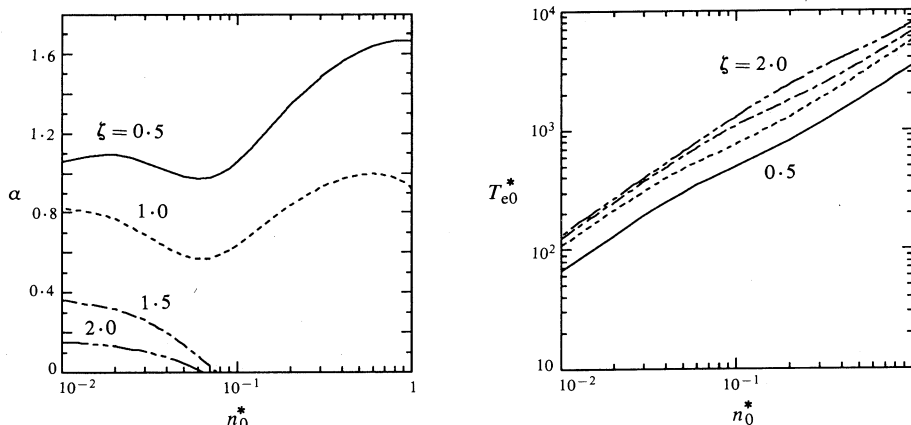

Fig. 6. The same as Fig. 5 except $R = 0 \cdot 5$ m.

However, using Figs 2–6 and other results, we have identified four parameter regions for which α is small:

(i)   When $T_{e0}^* < 20$ the energy loss is dominated by plasma recycling (P_{ne}). The fact that the expression for Γ_t given in equation (12) has to be multiplied by the small factor α to obtain $P_{ne} \approx P_{\Omega}$ probably indicates that, for these low temperature cases, the density gradient at the separatrix is not as large as the Ψ^2 model prediction.

(ii) When $20 < T_{e0}^* < 50$, the line radiation power from a 3% level of oxygen impurity can be similar to or larger than P_{Ω}, in which case $\alpha < 0$. This is illustrated by comparing Figs 2 and 3 with Fig. 4.

(iii) When $T_{e0}^* > 10^4$ the electron cyclotron power loss exceeds P_{Ω}, and $\alpha < 0$ (see Fig. 3). However, it should be remembered that (35) does not include any reabsorption of the electron cyclotron radiation by the plasma.
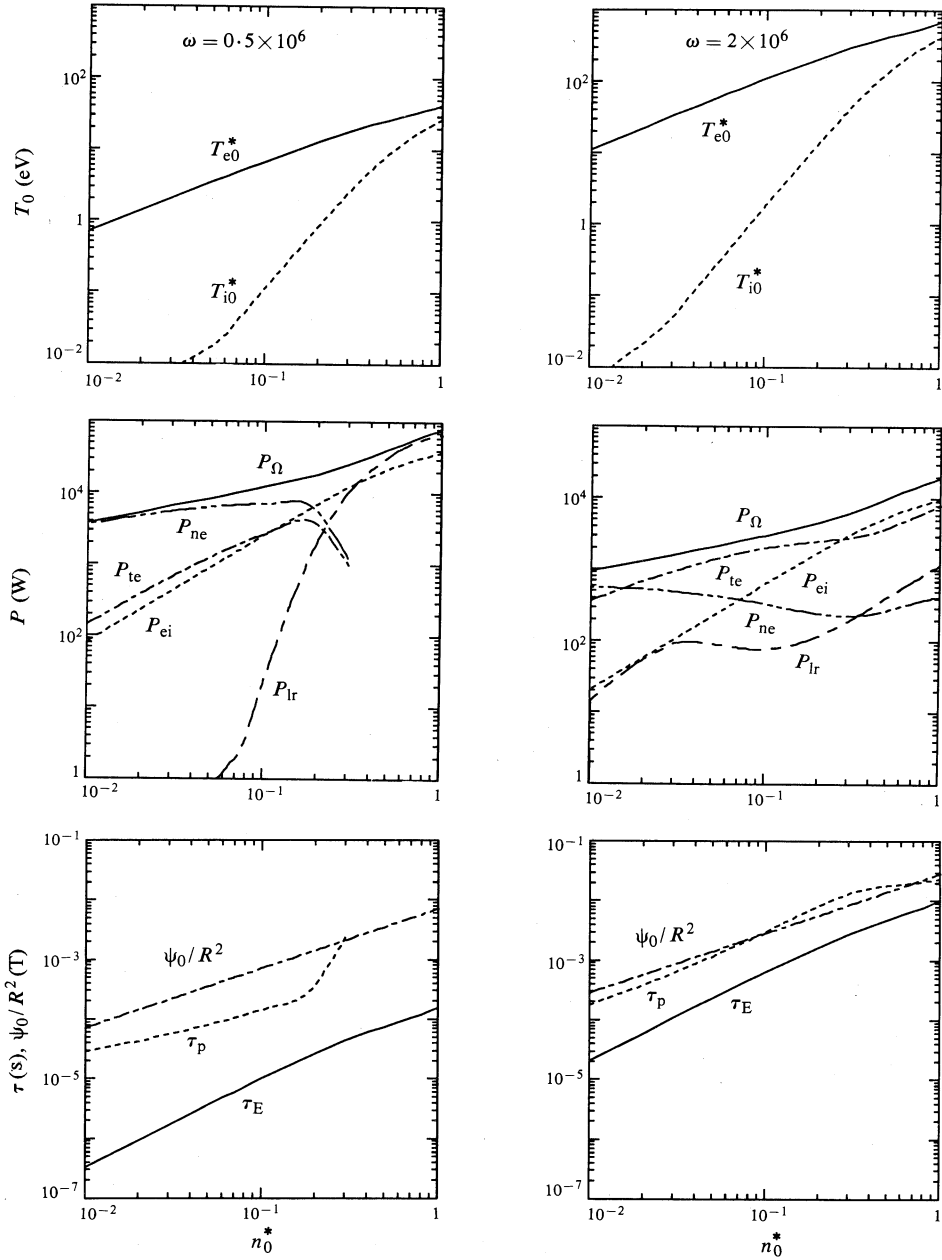
Fig. 7. Temperatures, power terms, confinement times and the magnetic field normalisation as a function of n_0^* for $R = 0.2$ m, $\zeta = 1$ and $\omega = 0.5 \times 10^6$ and 2×10^6 rad s^{-1}. The terms P_{ne}, P_{te} and τ_p are not shown when α is negative.

(iv)   Figs 5 and 6 show that α decreases and becomes negative as ζ increases. This is because of the rapid increase of $\mathscr{I}_{tr}$ with ζ. Equations (30), (31) and (33) show that an increasing $\mathscr{I}_{tr}$ can be compensated for by a decreasing but finite α as far as P_{te} and P_{ne} are concerned. Negative values of α arise because P_{ti} increases with $\mathscr{I}_{tr}$, and this leads to lower T_i and larger values of P_{ei}
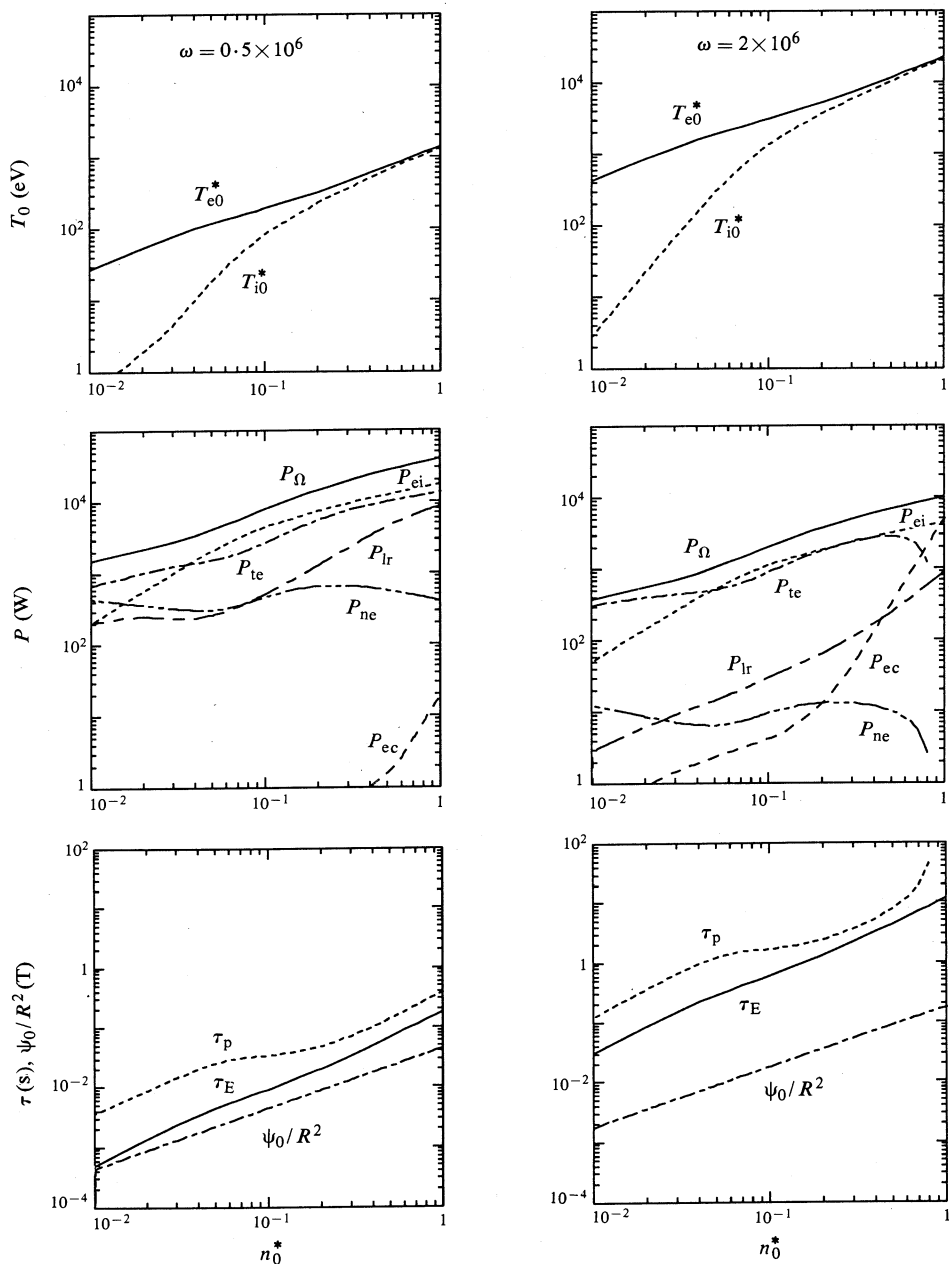
Fig. 8. The same as Fig. 7 except $R = 0.5$ m.

which exceed P_Ω. As discussed in Section 6, a more sophisticated evaluation of $\mathscr{I}_{tr}$ would probably predict $\mathscr{I}_{tr} \propto \zeta$; α would then be relatively independent of ζ.

For those cases in which α becomes small or negative, additional heating would have to be added to the plasma to enable power balance to be obtained for plasma configurations given by the Ψ^2 model.

In Figs 7 and 8 we show, for $\zeta = 1$ and different ω and R values, the plasma temperatures, the dominant power terms and the confinement times. Also shown is the magnetic field scaling factor ψ_0/R^2, which is given in equation (45). In all cases considered, we have found that P_{ti} dominates the ion energy loss, so that P_{ti} and P_{ei} are virtually identical. The following observations can be made:

(a)   At low densities the ion temperatures are very low. This occurs because P_{ei} is small, and because the small magnetic field allows large ion thermal energy losses. It is obvious that our model of a peaked ion temperature profile is nonphysical in these cases, and a more realistic model would have an almost constant ion temperature profile. At higher densities, P_{ei} is comparable with P_Ω and the larger magnetic fields reduce the ion thermal conductivity, which results in $T_i \rightarrow T_e$.

(b)   When $T^*_{e0} < 20$, the dominant energy loss mechanism comes from plasma recycling (P_{ne}). The electron thermal energy loss generally dominates when $20 < T^*_{e0} < 100$, and ion thermal energy loss ($P_{ti} \approx P_{ei}$) dominates at higher temperatures.

(c)   For given ω and R, the particle confinement times increase with density as n_0^δ with $1 < \delta < 1 \cdot 5$. For the small and cool plasmas, the confinement times appear reasonable when compared with the experimental values (Durance *et al.* 1987). However, when $T^*_{e0} > 10^3$, the predicted confinement times are quite large when compared with values obtained on devices such as tokamaks. It is possible that turbulent effects, for example the lower hybrid drift instability (Hoffman *et al.* 1984), will occur at these high temperatures and lead to loss rates greater than the 'enhanced classical' values of P_{te} and Γ_t used here. In such cases, additional heating would be needed to obtain the high temperature plasmas unless the turbulence also causes an anomalous resistivity and a sufficient increase in P_Ω.

9.   Analysis of Small Plasmas

Durance *et al.* (1987) have reported detailed measurements of a particular rotamak discharge in a spherical vessel with a 14 cm radius. The experimental density and temperature are much less peaked in the region of the magnetic axis than predicted by the Ψ^2 model. Nevertheless, using the n_0 and I_ϕ values measured in the experiment, the Ψ^2 model predicts $\tau_E \approx 10 \, \mu s$ which is in surprisingly good agreement with the measured value of about $5 \, \mu s$. We calculate that the dominant energy loss term is P_{ne}.

It is desirable to ascertain which configuration of the plasma optimises τ_E subject to the constraint that the separatrix is confined within a spherical vessel of radius R_c. Therefore, the variation with ζ of τ_E and other terms of interest is shown in Fig. 9 for $R_c = 0 \cdot 14$ and $0 \cdot 20$ m. The separatrix radius is given by

$$R = R_c, \quad \text{when} \quad \zeta \leqslant 1$$

$$= R_c/\zeta, \quad \text{when} \quad \zeta > 1.$$

Most terms vary only weakly with ζ for $\zeta < 1$, but change markedly when $\zeta > 1$. The optimum shape in this case is a spherical one. The degradation of confinement for the prolate configurations occurs because I_ϕ, T_0 and the magnetic field at the separatrix all decrease as ζ increases above 1. Fig. 9 also shows that significant increases in τ_E and T_0 can be achieved by enlarging R_c from $0 \cdot 14$ to $0 \cdot 20$ m, and that this is accompanied by a lowering of P_Ω. We remark that, for both radii and the
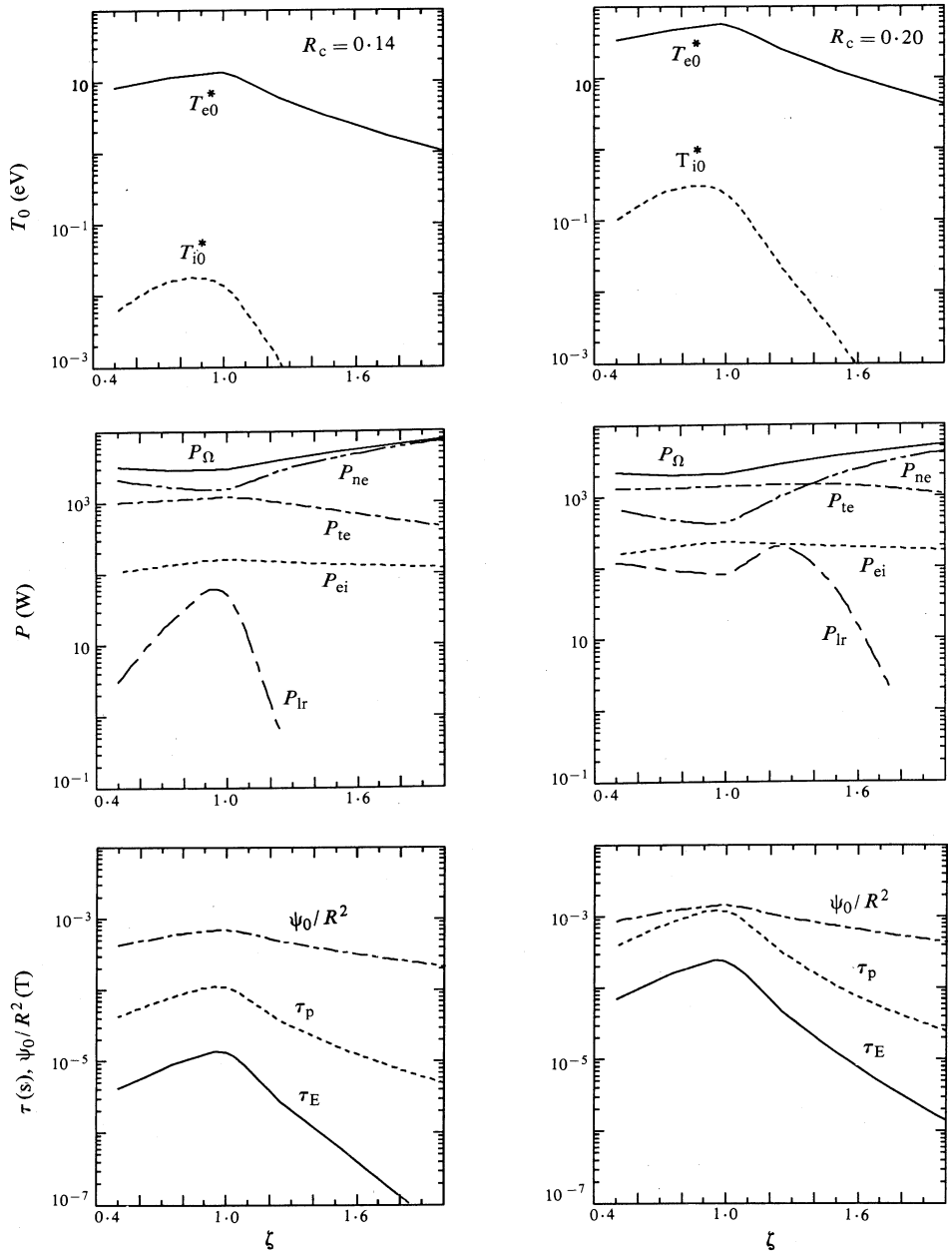
Fig. 9. Temperatures, power terms, confinement times and the magnetic field normalisation as a function of ζ for $n_0^* = 0 \cdot 05$, $\omega = 2 \times 10^6$ rad s^{-1} and vessel radii $R_c = 0 \cdot 14$ and $0 \cdot 20$ m.

range of n_0 and ω values considered, α typically decreases slowly as ζ increases from $0 \cdot 5$ to 1 and then decreases rapidly by a factor ~ 10 as ζ goes from 1 to 2. These calculations have been repeated with $R = R_c$ for all ζ. In this case we find that most terms have only a small dependence on ζ when $1 \leqslant \zeta \leqslant 2$. In particular, both P_Ω and τ_E increase by about 50% as ζ goes from 1 to 2. The ζ dependence of α and T_{e0} is indicated in Figs 5 and 6.

10. Discussion

For medium size plasmas with electron and ion temperatures around 100 eV and with fully penetrating low amplitude RMFs, we expect to obtain energy transfer rates that would be in reasonable agreement with experimental values, with the possible exception of the electron thermal conduction. However, in the lower temperature experiments that have been conducted (e.g. Durance *et al.* 1987) the following effects merit consideration:

(i) The RMFs are of similar amplitude to the steady fields. This could lead to a modified thermal conductivity. Such an effect is not necessarily deleterious because some preliminary theoretical work indicates that RMF current drive actually reduces particle diffusion (I. R. Jones, personal communication).

(ii) When the RMF does not fully penetrate the plasma, the frequency of the electron fluid rotation is less than ω. This 'slip' between the RMF and the electrons leads to a transfer of energy to the plasma at a rate larger than P_Ω (Hugrass 1984).

(iii) Measured density and temperature profiles are not as peaked as those given by the Ψ^2 model. Also, considerable plasma current exists outside the separatrix in some experiments.

(iv) The corona model may not accurately predict line radiation from impurities in experiments of short duration or with large particle fluxes.

Despite the fact that the Ψ^2 model describes existing experiments only approximately, it can be used to estimate the dominant energy loss terms for these and for projected experiments. Our main conclusions can be summarised as follows:

(a) As the plasma temperature increases, the dominant energy loss mechanism changes from plasma recycling to electron thermal conduction to ion thermal conduction. The presence of a 3% level of oxygen impurity can lead to domination of the energy loss by line radiation when $T_{e0} \sim 30$ eV.

(b) The prediction that $\tau_E \propto R^8$ indicates that significant improvement in plasma confinement can be obtained by increasing the plasma size provided that the thermal energy transport remains classical.

(c) If a spherical discharge vessel is used, the optimum plasma shape is also spherical. However, if the vessel is cylindrical with its axis larger than its diameter, prolate configurations may give slightly better τ_E values than spherical ones.

(d) In low current plasmas the small magnetic fields allow rapid loss of the ion thermal energy, and the electron–ion energy equilibration term is small. Consequently, we have $T_i \ll T_e$ and we expect the ion temperature profile to be fairly flat.

References

Abramowitz, M., and Stegun, I. A. (1965). 'Handbook of Mathematical Functions' (Dover: New York).

Auerbach, S. P., and Condit, W. C. (1981). *Nucl. Fusion* **21**, 927.

Braginskii, S. I. (1965). 'Reviews of Plasma Physics, Vol. 1 (Ed. M. A. Leonovich), p. 205 (Consultants Bureau: New York).

Dolan, T. J. (1982). 'Fusion Research', Vol. 1 (Pergamon: New York).

Donnelly, I. J., Rose, E. K., and Cook, J. L. (1987). *Aust. J. Phys.* **40**, 175.

Durance, G., Hogg, G. R., Tendys, J., and Watterson, P. A. (1987). Studies of equilibrium in the AAEC rotamak. *Plasma Phys. Contr. Fusion* (submitted).

Harrison, M. F. A. (1984). 'Applied Atomic Collision Physics', Vol. 2 (Eds H. S. W. Massey *et al.*), p. 395 (Academic: London).

Hinton, F. L. (1983). 'Handbook of Plasma Physics', Vol. 1 (Eds M. N. Rosenbluth and R. Z. Sagdeev), p. 147 (North-Holland: Amsterdam).

Hoffman, A. L., Harding, D. G., Milroy, R. D., Slough, J. T., Steinhauer, L. C., and Vlases, G. C. (1984). Proc. 10th Int. Conf. on Plasma Physics and Controlled Nuclear Fusion Research, London, Vol. 2, p. 601 (IAEA: Vienna).

Hugill, J. (1983). *Nucl. Fusion* **23**, 331.

Hugrass, W. N. (1984). *Aust. J. Phys.* **37**, 509.

Hugrass, W. N., Jones, I. R., McKenna, K. F., Phillips, M. G. R., Storer, R. G., and Tuczek, H. (1980). *Phys. Rev. Lett.* **25**, 1676.

Jones, I. R., and Hugrass, W. N. (1981). *J. Plasma Phys.* **26**, 441.

McKenna, K. F., Rej, D. J., and Tuszewski, M. (1983). *Nucl. Fusion* **23**, 1319.

Miyamoto, K. (1980). 'Plasma Physics for Nuclear Fusion' (MIT Press: Cambridge, Mass.).

Nguyen, K., and Kammash, T. (1982). *Plasma Phys.* **24**, 177.

Post, D. E., Jensen, R. V., Tarter, C. B., Grasberger, W. H., and Lokke, W. A. (1977). *At. Data Nucl. Data Tables* **20**, 5.

Solov'ev, L. S. (1975). 'Reviews of Plasma Physics', Vol. 6 (Ed. M. A. Leonovich), p. 239 (Consultants Bureau: New York).

Appendix.   Solov'ev Model Energy Transfer

The Solov'ev model equilibrium discussed in DRC is now used to evaluate the particle flux and the power terms which are defined in Sections 3 and 4 (P_Ω is infinite because of the infinite ohmic heating power density at the separatrix):

$$\Gamma_{\mathrm{t}} = 6 \cdot 5 \times 10^{23} \psi^{-\frac{3}{2}} (4 + \zeta^{-2}) n_0^* (T_{\mathrm{i0}}^* - 0 \cdot 5 \, T_{\mathrm{e0}}^*)(T_0^*)^{-1}$$

$$\times \, (T_{\mathrm{e0}}^*)^{-\frac{3}{2}} R \mathscr{I}_{\mathrm{tr}}, \tag{A1}$$

$$P_{\mathrm{ei}} = 7 \cdot 5 \times 10^7 (n_0^*)^2 (T_{\mathrm{e0}}^*)^{-\frac{3}{2}} (T_{\mathrm{e0}}^* - T_{\mathrm{i0}}^*) R^3 \mathscr{I}_{1,-1}, \tag{A2}$$

$$P_{\mathrm{te}} = 2 \times 10^5 \psi^{-\frac{1}{2}} (4 + \zeta^{-2}) n_0^* (T_{\mathrm{e0}}^*)^{-\frac{1}{2}} R \mathscr{I}_{\mathrm{tr}}, \tag{A3}$$

$$P_{\mathrm{br}} = 150 Z_{\mathrm{eff}} (n_0^*)^2 (T_{\mathrm{e0}}^*)^{\frac{1}{2}} R^3 \mathscr{I}_{11}, \tag{A4}$$

$$P_{\mathrm{ec}} = 1 \cdot 6 \times 10^{-5} (4 + \zeta^{-2})^{-1} (n_0^*)^2 \, T_{\mathrm{e0}}^* \, T_0^* \, R^3 \mathscr{I}_{\mathrm{ec}}, \tag{A5}$$

$$P_{\mathrm{lr}} = 10^{40} f_{\mathrm{ox}} (n_0^*)^2 R^3 \mathscr{I}_{\mathrm{lr}}, \tag{A6}$$

$$P_{\mathrm{ti}} = 6 \cdot 4 \times 10^6 \psi^{-\frac{1}{2}} (4 + \zeta^{-2}) n_0^* (T_{\mathrm{i0}}^*)^{\frac{1}{2}} (T_0^*)^{-1} R \mathscr{I}_{\mathrm{tr}}, \tag{A7}$$

and P_{ne} and P_{cx} can be obtained using (A1).

The integrals $\mathscr{I}_{mn}$, defined in equation (26), have the values

$$\mathscr{I}_{mn} = 2^{2n+1}\pi B\left(\frac{n+2}{2}, \frac{n+2}{2}\right) B\left(\frac{m+n+1}{2}, \frac{n+3}{2}\right)\zeta, \qquad (A8)$$

where $B(x, y)$ are the beta functions (Abramowitz and Stegun 1965). Specifically, we have

$$\mathscr{I}_{1,-1} = 9 \cdot 87\zeta, \quad \mathscr{I}_{11} = 2 \cdot 63\zeta, \quad \mathscr{I}_{12} = 1 \cdot 92\zeta; \qquad (A9)$$

$$\mathscr{I}_{ec} = 4\pi \int_0^\zeta dZ \int_0^{X'} X^{-1}\left\{\left(\frac{\partial\psi}{\partial X}\right)^2 + \left(\frac{\partial\psi}{\partial Z}\right)^2\right\}\psi\, dX$$

$$= 19 \cdot 8\zeta + 5 \cdot 0\zeta^{-1}; \qquad (A10)$$

$$\mathscr{I}_{lr}(T_{e0}) = 4\pi\zeta \int_0^1 dZ \int_0^{X'} X R_{ox}(T_{e0}\,\psi)\, dX, \qquad (A11)$$

where the integral is evaluated using ψ with $\zeta = 1$.

We define

$$\mathscr{I}'_{tr}(X) = 4\pi \int_0^{l(X)} X^3\left\{\left(\frac{\partial\psi}{\partial X}\right)^2 + \left(\frac{\partial\psi}{\partial Z}\right)^2\right\}^{-\frac{1}{2}} dl$$

$$= 0 \cdot 5\pi\{1 - (1-X^2)^{\frac{1}{2}}\}\zeta, \qquad (A12)$$

and therefore

$$\mathscr{I}_{tr} = \mathscr{I}'_{tr}(1) = 0 \cdot 5\pi\zeta. \qquad (A13)$$

Also, the contribution to $\mathscr{I}_{tr}$ from the region $X \leqslant 0 \cdot 5$ is proportional to X^2 and is small.

Because n is constant in this model, the dependence on ψ of the particle and thermal energy transport terms is quite different from that of the Ψ^2 model. Also, we note that (A1) predicts a negative Γ_t if $T_{e0} > 2T_{i0}$.